Case Studies in the Application of Raman Microscopy

The authors discuss how the Raman microscope is being used successfully to characterize pharmaceuticals, analyze disease states, and to characterize semiconductors and nanotechnologies.

Fran Adar, Coralie Naudin, and Andrew Whitley

The introduction of the Raman microprobe in the early- to mid-1970s (1) truly was an innovation in simplifying Raman sampling, which provided the additional advantages of confocality and fluorescence rejection. While its application to materials problems was instrumental in widening the use of Raman, the technique really didn't become widely used until the reduction of the size of the instrumentation during the 1990s (2). This was due to the introduction of the holographic notch filter to separate the Raman signal from the unshifted laser radiation, air-cooled lasers, low noise, CCD detectors, and powerful desktop computers with mature software.

From the mid-1990s until the present the application of Raman instrumentation to ever-expanding materials studies has created a ground-swell of interest. During this period, the availability of Fourier-transform (FT) Raman instrumentation in the analytical community gave the technology credibility that continued to fuel this growth. However, the application of FT-Raman spectroscopy to problem solving apparently has peaked, and now is in decline. But in its wake the reluctance of the analytical community to employ Raman spectroscopy to solve its problems has been removed (3). Because of this enthusiasm, the equipment manufacturers have provided more and more specialized developments for targeted real-world applications. The remainder of this article will discuss some of these applications.

Characterization of Pharmaceuticals

With the large amount of time required between identifying a pharmaceutical need and introducing a drug to market, and the associated costs for all steps of this process, any technologies that can assist at any step can be of interest. Raman is being explored early in the process as a means of understanding the disease process at the molecular level (see the next section). But it also is being exploited in characterizing materials at every step in drug development. Both small molecules and larger active agents

Fran Adar is worldwide Raman applications manager, **Coralie Naudin** is a Raman application engineer, and **Andrew Whitley** is director, Raman Division, for Jobin Yvon (Edison, NJ). E-mail: Fran.Adar@JobinYvon.com.

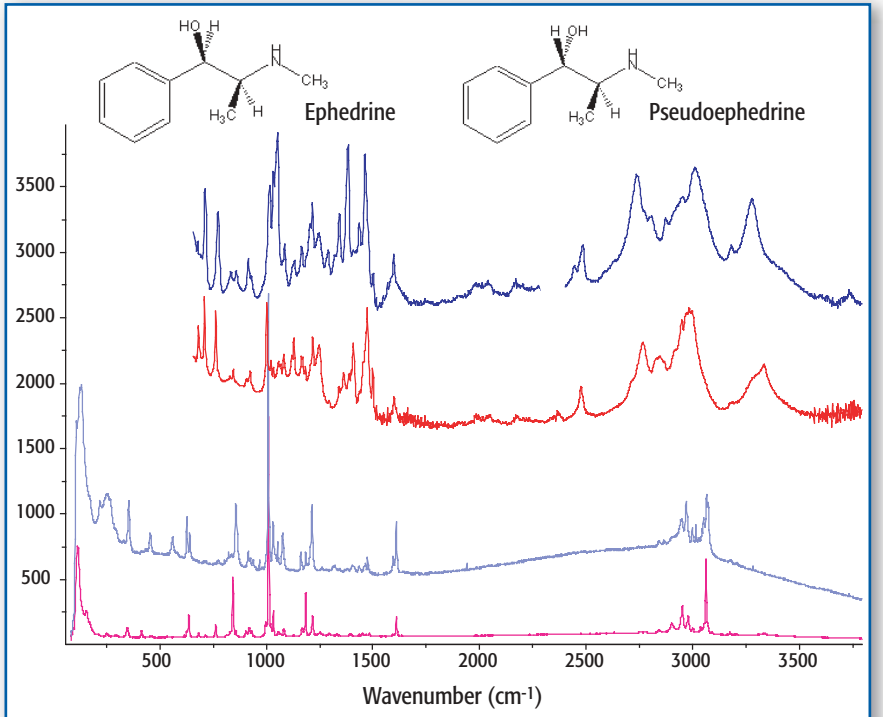

Figure 1. FT-IR (top) and Raman (bottom) microprobe spectra of ephedrine and pseudoephedrine recorded on the LabRAM-IR™. In each pair, the ephedrine spectrum appears below the pseudoephedrine spectrum.

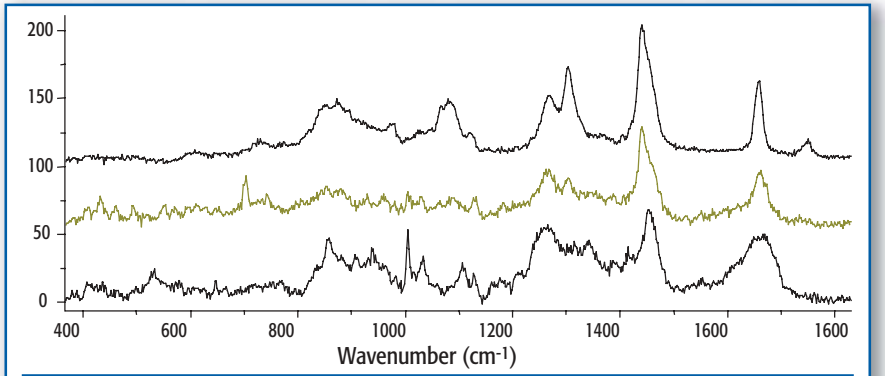

Figure 2. Raman microscope spectra (from top to bottom) of fat cell, globule in protein region, and protein region.

such as proteins can be characterized by their vibrational spectra. For instance, the spectra of molecules that only differ by the configuration at one chiral center can be differentiated. Figure 1 shows the spectra of ephedrine and pseudoephedrine where the differences are clearly visible. In contrast the molecules differ only in the configuration of the chiral center next to the aromatic ring.

The high information content of vibrational spectra is being exploited in the reaction chemistry of the active pharmaceutical ingredient (API), during formulation (mixing with excipients), and for mapping the various species in final tablets. However, another application is experiencing widespread use where the equipment has been modified significantly to accommodate the application. That application is polymorph screening.

Small organic molecules can crystallize in multiple polymorphic forms, some of which include solvent molecules; when the solvent is water, the forms are called "pseudomorphs." The polymorphic forms affect solubility, bioavailability, stability (including capacity for water uptake), and so forth. For these reasons, the polymorphic form also is included in the patent protection of the drug. For polymorphic screening the LabRAM (Jobin Yvon, Villeneuve d'Ascq, France) is used with a large motorized stage (*x*, *y*, and *z* control) and has software modified for automated crystal location and spectral acquisition. The Crystal iD (Jobin Yvon, Villeneuve d'Ascq, France) software includes pattern recognition of the optical images, incorporating algorithms developed, in collaboration with a major drug manufacturer, by Imaging Associates in the UK.

Molecular Characterization of Metabolic and Disease States

Molecular definition of foreign materials and/or metabolic accretions and creation of maps correlated to white light microscopy have been performed successfully for a number of years (4). Because molecular changes precede visible histological changes in diseased tissue, numerous workers have been utilizing Raman microscopy to determine if disease state markers can be identified (5, 6). In our own laboratory we have collaborated with Rousseau and Yeh at the Albert Einstein School of Medicine on an apoE knock-out mouse model of human atherosclerosis (7). In addition to similar observations to what other workers are reporting for this disease process, we observed free fatty acid inclusions in the knock out mouse, and calcification in the form of calcite ($CaCO_3$) in a very old normal (wild type) mouse. One might assume that the first observation is relevant to the disease process itself. The second may be related to reduced availability or activity of carbonic anhydrase in the aged animal.

In Figure 2, the strong band at 1650 cm^{-1} is assigned to the >C=C< unsaturation bond of the lipids. When esterified the >C=O group has a well-defined band at about 1750 cm^{-1}. The bottom spectrum is a typical protein spectrum and shows a fairly broad amide I band near 1650 cm^{-1} (not be to confused with the sharper carbon double bond) and a sharp aromatic band at 1000 cm^{-1}. The middle spectrum is the anomaly. The 1650 cm^{-1} band is too sharp for a protein suggesting that it could arise from the unsaturated lipid. But the carbonyl band at 1750 cm^{-1} is lacking, suggesting that the carboxylate group is unesterified.

Another area of development is the definition enzyme/protein allotrope for selection of optimized drug for disease

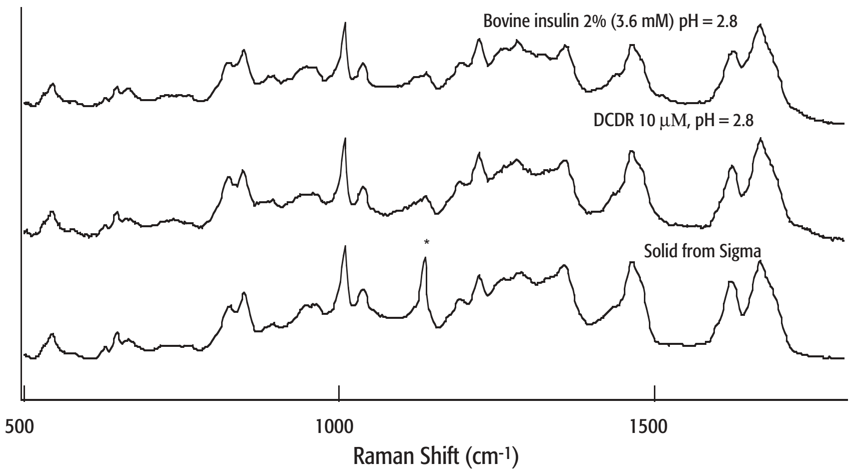

Figure 3. Raman spectrum of bovine insulin acquired from a 2% solution (3.6 µM) at pH 2.8 (top), drop coating deposition Raman (DCDR) spot deposited from 10 µM solution, also pH 2.8 (middle), and solid material (bottom).

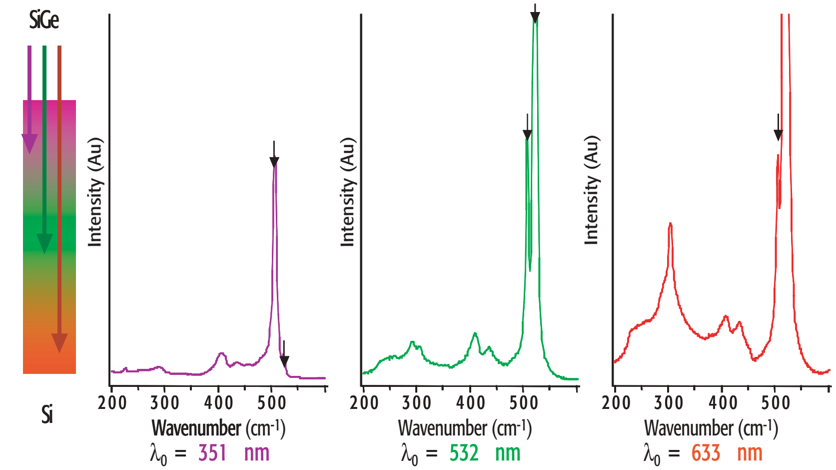

Figure 4. Raman spectra of a Si over SiGe layer generated by excitation wavelengths of 351 nm (left), 532 nm (middle) and 633 nm (right). The rectangle on the far left indicates schematically the depth to which the laser excitation can penetrate (not to scale).

treatment. Because assaying serum and cell isolates often involves working with very small amounts of material, analysis can be difficult. The group of Dor BenAmotz at Purdue University has shown that Raman spectra are sensitive to subtle molecular differences such as posttranslational glycosylation and phosphorylation, and small amino acid differences in proteins such as insulin from various sources. In addition, this group has developed hydrophobic substrates that enable deposition of detectable amounts of material precipitated from microliter droplets from solutions as dilute as 10 µM (8). These substrates are called SpectRIM slides (Tienta Sciences, Indianapolis, IN).

The spectra shown in Figure 3 demonstrate that this technique provides accurate Raman spectra of very small amounts of material (as little as 25 fmol) with conformation and degree of hydration not much different from that of dissolved or lyophilized material. As an added benefit, it has been observed that the deposition of the droplet and subsequent evaporation provides segregation of species with subsequent purification. The starred peak at the bottom of the figure is assigned to an impurity in the lyophilized material that appears neither in the solution spectrum or that of the dried material. In fact, because proteins tend to be less soluble than buffering agents, the protein precipitates out as a ring inside of which the buffer molecules can be found. This also means that fluorescing impurities sometimes are separated from the sample of interest.

Characterization of Nanotubes and Measurement of Stress in Integrated Circuits

Current developments in the design of integrated circuits are targeted on increasing the integration scale and speed of devices. Silicon-on-insulator enables electrical isolation of the surface devices from the substrate, which reduces the capacitance of the devices and the possibilities for shorts. Si on SiGe produces stress in silicon, which increases the electronic mobility in a controlled manner. And there even is development of a combination of the two technologies. Raman has been shown to be a useful tool for measuring stress in situ, non-destructively with microscopic spatial resolution. There is a concern, however, how to separate the shift of the Raman line due to stress and to Ge content. This has been worked out by Tsang and involves making simultaneous measurements of the Si–Si line (500–520 cm^{-1}) and the SiGe line (ca. 400 cm^{-1}) and solving an equation that appears in his publication (9). In addition, when there is a silicon layer overcoating a SiGe layer, it is possible to separate the contributions of the various layers by varying the excitation wavelength, which controls the depth of penetration of the laser beam.

Figure 4 shows the spectra of a sample of SiGe deposited on Si (the opposite of what is described above) when excitation wavelengths of 633, 532, and 325 nm were used. Inspection of the figure indicates that excitation with longer wavelength lasers give comparatively higher contributions from the silicon substrate whose frequency is closer to that of pure, unstressed silicon (520.6 cm^{-1}) than that of the SiGe layer. It even is possible to map these layers — and the map can represent any of the physical parameters of the film. In addition to being able to map intensity it is possible to map the frequency, which is related directly to germanium composition and stress. Figure 5 illustrates these mapping capabilities.

Carbon nanotubes is another area exhibiting very high interest for mate-

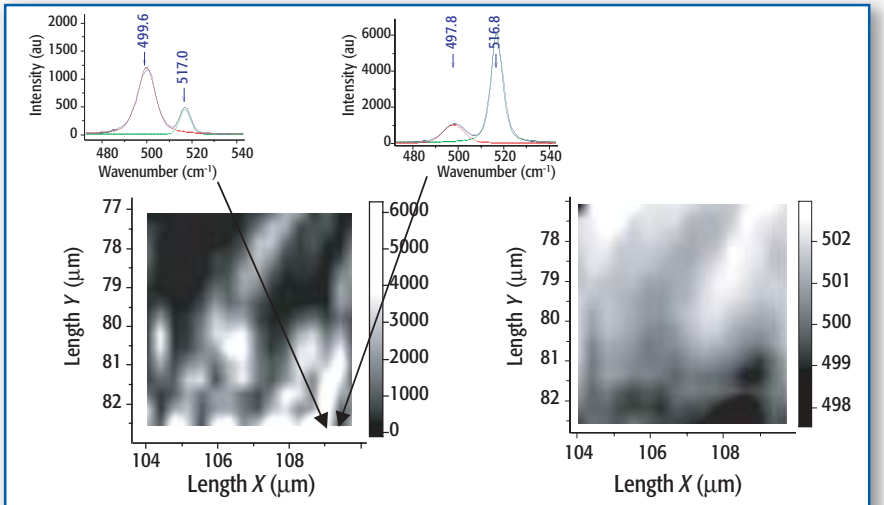

Figure 5. Raman maps of (left) the intensities of the silicon line from the substrate (light) vs. the SIGe cap layer (dark) and (right) the frequency of the Si–Si line in the SiGe layer.

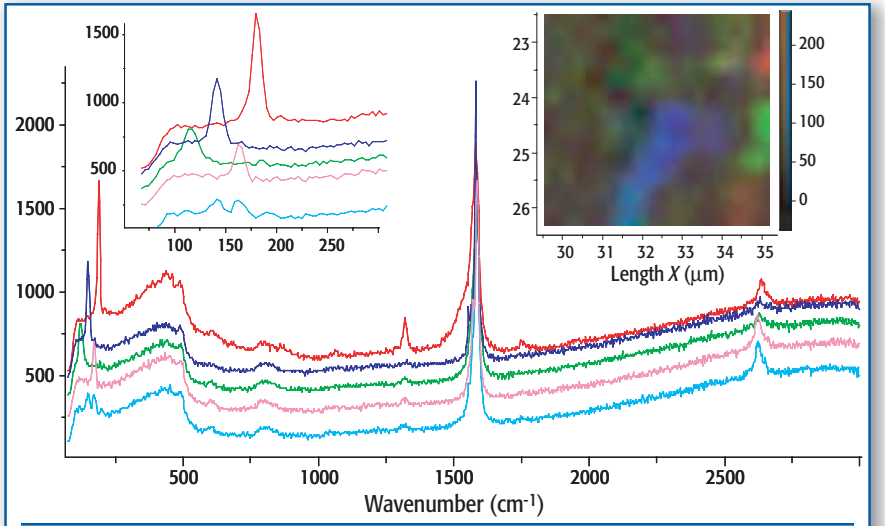

Figure 6. Five Raman microprobe spectra extracted from a map of single-walled nanotubes (SWNTs) recorded with 0.3-µm steps. The inset on the upper left shows the spectra expanded in the radial breathing mode (RBM) region. The inset on the upper right shows a map of these species, color coded as in the spectra.

rials development where Raman spectroscopy sometimes is the technique of choice for characterizing these materials. Carbon nanotubes are of interest for their electronic, mechanical, and chemical properties. Applications under consideration are electronic devices, composites, and drug delivery. A full analysis of the normal coordinates of the tubes and their resonance enhancement properties indicates that it is possible to identify the tube type from the Raman spectra (10). But this requires a range of excitation wavelengths and access to at least 100-cm^{-1} shift from the laser line. Incredibly, the sensitivity is adequate to detect and identify individual single walled nanotubes whose diameters are of the order of 5–10 nm. Figure 6 shows the result of a map of a sample with a mixture of single walled nanotubes. The fact that most spectra in the map show only one line in the region of the radial breathing mode implies that sensitivity is adequate to detect one tube.

Summary

It is clear that Raman microscopes have an important role to play in the evolution of new state-of-the-art technologies. The examples described above were selected for the high profile that these developments currently have.

References

1. M. Delhaye and P. Dhamelincourt, Raman Microprobe and Microscope with Laser Excitation, *J. Raman Spectrosc.* **3**, 33–43 (1975).
2. Evolution and Revolution of Raman Instrumentation — Application of Available Technologies to Spectroscopy and Microscopy, F. Adar, Chapter 2 in *Handbook of Raman Spectroscopy*, I.R. Lewis and H.G.M. Edwards, eds. (Marcel Dekker, New York, 2001).
3. Fourier-Transform Raman Spectroscopy: From Concept to Experiment, B. Chase, in *Fourier Transform Raman Spectroscopy,* D.B. Chase and J.F. Rabolt, eds. (Academic Press, San Diego, 1994).
4. J.A. Centeno, K.G. Ishak, F.G. Mullick, W.A. Gahll, and T.J.O'Leary, *Appl. Spec.* **48**, 569–572 (1994); J.P. Pestaner, F.G. Mullick, F.B. Johnson, and J.A. Centeno, *Aarch Pathol Lab Med*, **120**, 537–540 (1996); and J.A. Centeno, F.G. Mullick, R.G. Panops, F.W. Miller and A. Valenzuela-Espinoza, *Modern Pathology* **12**, (7) 714–720 (1999).
5. C. Otto, C.J. deGrauw, J.J. Duindam, N.M. Sijtsema, and J. Greve, *J. Raman Spectrosc.* **28**, 143–150 (1997); and P.J. Caspers, G.W. Lucassen, E.A. Carter, H.A. Bruining, and G.J. Opuppels, *J. Investigative Dermatology* **116**,(3) 434–442 (2001).
6. E.B. Hanlon, R. Manoharan, T.W. Koo, K.E. Shafer, J.T. Motz, M. Fitzmaurice, J.R. Kramer, I. Itzkan, R.R. Dasari, and M.S. Feld, *Physics in Medicine and Biology* **45**(2), R1 (2000).
7. F. Adar, L. Jelicks, C. Naudin, D. Rousseau, S. Yeh, Elucidation of the Atherosclerotic Disease Process in Apo E and Wild Type Mice by Vibrational Spectroscopy, SPIE 5321A-11, January, 2004.
8. D. BenAmotz, *Anal. Chem.* **75** 5703–5709 (2003).
9. J. Tsang, P.M. Mooney, F. Dacol, and J.O. Chu, *J. Appl. Phys.* **75**(12), 8098–8108 (1994).
10. M.S. Dresselhaus and P.C. Eklund, *Adv. in Physics* 49/6, 705–814 (2000). ■